

Article

Sustainable Route for Synthesis of All-Silica SOD Zeolite

Hangling Zhai ¹, Chaoqun Bian ², Yuxia Yu ¹, Longfeng Zhu ^{1,*} , Lingfeng Guo ¹, Xiao Wang ¹, Qinqin Yu ¹, Jie Zhu ¹ and Xuebo Cao ^{1,*}¹ College of Biological, Chemical Sciences and Engineering, Jiaying University, Jiaying 314001, China² Pharmaceutical and Material Engineering School, Jinhua Polytechnic, Jinhua 321000, China* Correspondence: zhulf1988@mail.zjxu.edu.cn (L.Z.); xbciao@mail.zjxu.edu.cn (X.C.);
Tel.: +86-573-8364-0131 (L.Z. & X.C.)

Received: 19 June 2019; Accepted: 28 June 2019; Published: 30 June 2019



Abstract: The development of the sustainable synthesis of zeolites has become a very hot topic in recent years. Herein, we report a sustainable route for synthesizing all-silica SOD zeolite under solvent-free conditions. The method of solvent-free synthesis includes mixing, grinding, and heating raw solids. The all-silica SOD zeolite obtained was well characterized by multiple measurement techniques (XRD, SEM, IR, thermogravimetric-differential thermal analysis (TG-DTA), and magic angle spinning nuclear magnetic resonance (MAS NMR)). The crystallization process of all-silica SOD zeolite was also investigated in detail by XRD, SEM, UV-Raman, and MAS NMR techniques. In addition, the effects of the crystallization compositions, including the molar ratios of Na₂O/SiO₂ and ethylene glycol/SiO₂, on the synthesis of the pure all-silica SOD zeolite were investigated at different temperatures.

Keywords: zeolite; sustainable route; all-silica SOD; solvent-free synthesis

1. Introduction

Zeolites, which are constructed by AlO₄ or SiO₄ tetrahedra, have been widely applied in gas adsorption and separation, ion exchange, and shape-selective catalysis [1–8]. To date, there are many zeolites that have been successfully synthesized including silicate, aluminosilicate, germanosilicate, and so on [1–8]. Silicate (all-silica) zeolites, as an important family of zeolites, have been used as catalytic supports, low-k dielectric materials, and adsorbents due to their strong hydrophobicity, high hydrothermal and thermal stability, and dielectric properties [6–13]. For example, all-silica Beta zeolite as a catalytic support showed excellent performance in formaldehyde combustion at room temperature [11]; silicalite-1 zeolite as an adsorbent demonstrated good adsorption of volatile organic compounds [12]; and silicalite-2 zeolite as a low-k dielectric material exhibited a promising ultra-low dielectric constant [13].

The all-silica SOD zeolite, firstly synthesized under solvothermal conditions by Bibby in 1985, is a promising candidate for the above applications. It is worth noting that a large amount of ethylene solvents were necessary in the synthesis, which acted as both an organic template and solvent [14–16]. Later, Gies et al. also reported that all-silica SOD zeolite was synthesized in the presence of pyrrolidine and ethylamine under solvothermal conditions [17]. Notably, a large amount of organic solvent was necessary in the process of all-silica SOD zeolite synthesis, which not only increased the production cost, but also produced polluted waste and thus led to the issue of environmental hazard. Therefore, it is highly desirable to develop a sustainable route for all-silica SOD zeolite synthesis.

Recently, a solvent-free method has been reported for synthesizing zeolites by mixing, grinding, and heating raw solids, which is regarded as a sustainable route. To date, various zeolites,

such as MFI, Beta, FAU, and MOR, have been successfully prepared under this route [18–22]. However, the synthesis of all-silica SOD zeolite has not yet been successful using this sustainable route. In this work, for the first time, we show a sustainable route for synthesizing all-silica SOD zeolite. The synthesis is well characterized by X-ray diffraction (XRD), scanning electron microscopy (SEM), thermogravimetric-differential thermal analysis (TG-DTA), infrared spectroscopy (IR), UV-Raman, and magic angle spinning nuclear magnetic resonance (MAS NMR).

2. Materials and Methods

2.1. Materials

Ethylene glycol (EG, 98%, Aladdin Chemistry Co., Ltd., Shanghai, China), solid silica gel (SiO_2 , 98%, Qingdao Haiyang Chemical Reagent Co., Ltd., Qingdao, China), and sodium metasilicate nonahydrate ($\text{Na}_2\text{SiO}_3 \cdot 9\text{H}_2\text{O}$, 98%, Aladdin Chemistry Co., Ltd., Shanghai, China) were used without further purification.

2.2. Synthesis

In a typical example of synthesizing the all-silica SOD zeolite, 0.5 g of $\text{Na}_2\text{SiO}_3 \cdot 9\text{H}_2\text{O}$, 1.57 g of SiO_2 , and 2.6 g of ethylene glycol were added into a mortar one by one and mixed together uniformly. After grinding for 15 min at room temperature, the powder was transferred to a 15 mL autoclave and sealed. After crystallization at 200 °C for 24 h, the product was fully crystalline. After filtering, washing with water at room temperature, and drying at 100 °C for 12 h, the final product was obtained, yielding a 1.75 g sample. This sample is denoted as S–Si–SOD.

2.3. Characterization

The X-ray diffraction (XRD) patterns were measured with a Rigaku Ultimate VI X-ray diffractometer (40 kV, 40 mA, Rigaku, Tokyo, Japan) using $\text{CuK}\alpha$ ($\lambda = 1.5406 \text{ \AA}$) radiation. Scanning electron microscopy (SEM) experiments were performed on Hitachi SU-1510 electron microscopes (Hitachi, Tokyo, Japan). The Fourier transform infrared spectroscopy (FTIR) spectra were recorded using a Bruker 66 V FTIR spectrometer (Bruker, Karlsruhe, Germany). UV-Raman spectra were measured with a Jobin-Yvon T64000 triple-stage spectrometer (Jobin-Yvon, Paris, France) with a spectral resolution of 2 cm^{-1} . The laser line at 325 nm of a He/Cd laser was used as an excitation source with an output of 50 mW. The power of the laser at the sample was about 3.0 mW. ^1H - ^{13}C CP/MAS NMR experiments were performed on a Bruker AVANCE-III 500 spectrometer (Bruker, Karlsruhe, Germany) using a 1.9 mm MAS probe with a sample spinning rate of 30 kHz; a total of 30,000 scans were accumulated with a recycle time of 5 s. Single-pulse ^{29}Si MAS NMR experiments with ^1H decoupling were performed on a Bruker AVANCE-III 500WB spectrometer (Bruker, Karlsruhe, Germany) using a 7 mm probe with a $\pi/4$ pulse width of 4.0 μs , a 60 s pulse delay, and a spinning rate of 4 kHz. TG-DTA analysis was carried out with a NETZSCH STA 449C (Netzsch, Bavaria, Germany) in air at a heating rate of 10 °C/min from room temperature to 800 °C.

3. Results and Discussion

3.1. Synthesis and Characterization of S–Si–SOD Zeolite

Figure 1 displays the XRD pattern of the as-made S–Si–SOD zeolite crystallized for 24 h at 200 °C under solvent-free conditions, giving a series of typical peaks associated with the SOD structure, in good agreement with the reported literature [14–16]. Figure 2 shows the different magnification SEM images of the as-made S–Si–SOD zeolite, which exhibits a blocky crystal morphology with a size of about 10 μm . Figure 3 shows the ^{29}Si MAS NMR spectrum of the as-made S–Si–SOD zeolite, giving three peaks with chemical shifts at around -117.2 , -110.3 , and -102.0 ppm. The peaks at

about -117.2 and -110.3 ppm are assigned to the Q^4 silica species ($Si(OSi)_4$), and the peak at about -102.0 ppm is assigned to the Q^3 silica species ($Si(OSi)_3(OH)$).

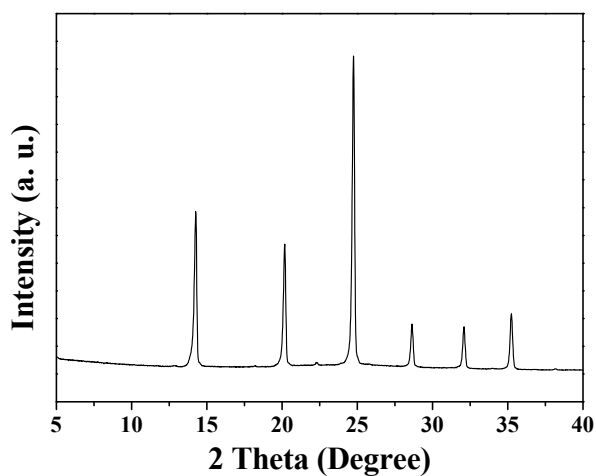


Figure 1. XRD pattern of the as-made S-Si-SOD zeolite synthesized at 200 °C.

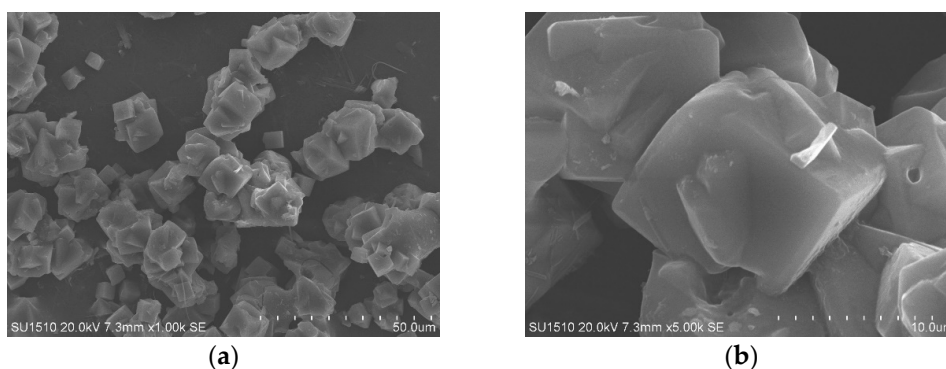


Figure 2. (a) Low magnification and (b) high magnification SEM images of the as-made S-Si-SOD zeolite synthesized at 200 °C.

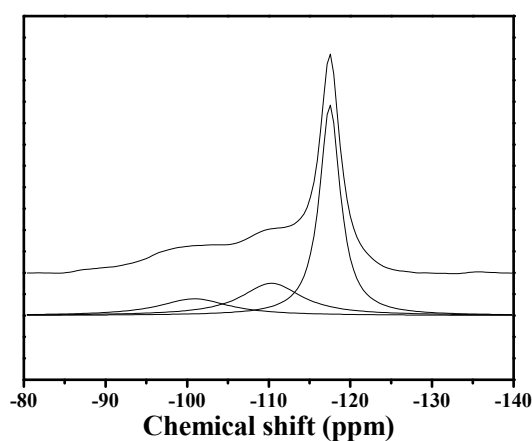


Figure 3. ^{29}Si MAS NMR spectrum of the as-made S-Si-SOD zeolite synthesized at 200 °C.

Figure 4a shows the ^{13}C MAS NMR spectrum of the as-made S-Si-SOD zeolite, giving the only one peak centered at about 64.0 ppm, which is assigned to the presence of ethylene glycol in the product. Figure 4b displays the IR spectra of the as-made S-Si-SOD zeolite. From Figure 4b, two bands at 2800 – 3000 cm^{-1} and one band centered at about 3440 cm^{-1} can be seen, which are assigned to the

ethyl group and hydroxyl group, respectively. Figure 4c shows the TG-DTA of the as-made S-Si-SOD zeolite, which gives the major exothermic peak at about 300–500 °C accompanied by a weight loss at about 5.8%, which is attributed to the decomposition of ethylene glycol in the S-Si-SOD zeolite framework. The above results support that the ethylene glycol is indeed used as an organic template to direct the formation of the S-Si-SOD zeolite.

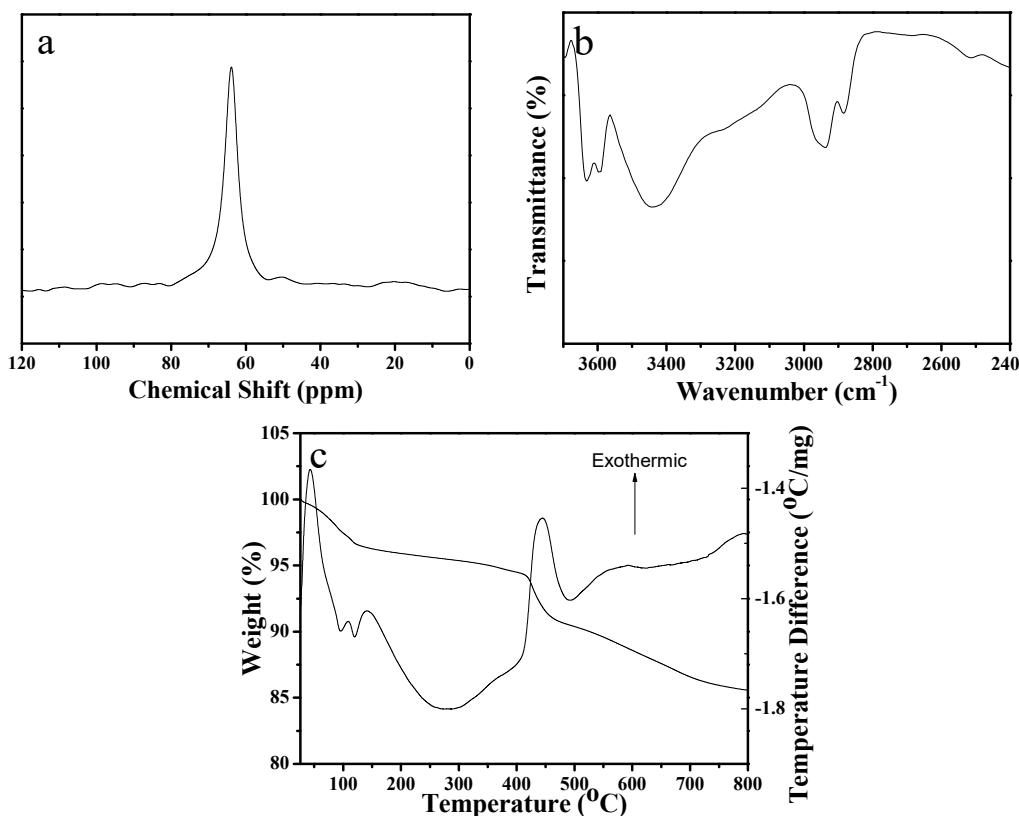


Figure 4. (a) ^{13}C MAS NMR spectrum, (b) IR spectrum, and (c) TG-DTA curves of the as-made S-Si-SOD zeolite synthesized at 200 °C.

3.2. Critical Factors for Synthesizing S-Si-SOD Zeolite

In the preparation process of S-Si-SOD zeolite, various factors influence the results of crystallization, such as the ratios of $\text{Na}_2\text{O}/\text{SiO}_2$, EG/SiO_2 and the synthesis temperature. Notably, the ratio of $\text{Na}_2\text{O}/\text{SiO}_2$ was very crucial to the synthesis of the final product. When the $\text{Na}_2\text{O}/\text{SiO}_2$ ratio was 0.01, the product was always amorphous (Table 1, Run 1, Figure 5a). Increasing the ratio of $\text{Na}_2\text{O}/\text{SiO}_2$ to 0.04, the S-Si-SOD zeolite product was dominant together with some amorphous phase (Table 1, Run 2, Figure 5b). Further increasing the ratio of $\text{Na}_2\text{O}/\text{SiO}_2$ to 0.06, the S-Si-SOD zeolite product with high crystallinity could be successfully obtained (Table 1, Run 3, Figure 1). However, a higher $\text{Na}_2\text{O}/\text{SiO}_2$ ratio would lead to the production of some amorphous phase again (Table 1, Run 4, Figure 5c). In addition, the ratio of EG/SiO_2 was also a very important factor for crystallization. When EG was absent in the starting mixture, the quartz and amorphous phase was always obtained (Table 1, Run 5, Figure 5d). When the EG/SiO_2 ratio was 1.0, the S-Si-SOD would be obtained accompanied by some amorphous phase (Table 1, Run 6, Figure 5e). Moreover, the influence of temperature on crystallization was also investigated. When the temperature was 160 °C, the product obtained was the amorphous phase (Table 1, Run 7, Figure 5f). When the temperature was 230 °C, the S-Si-SOD zeolite product could be obtained and the crystallization time was significantly decreased (Table 1, Run 8, Figure 5g). Furthermore, it was found that the addition of seed in the initial mixture also influenced the crystallization. When seed added it, the crystallization time greatly decreased and it only required 3 h (Table 1, Run 9, Figure 6a). More interestingly, the size of the S-Si-SOD zeolite was

about 1–2 μm , which was significantly smaller than that of the product without the addition of seed (Figure 6b).

Table 1. Synthesis of S–Si–SOD zeolite product under various conditions.

Run	Na ₂ O/SiO ₂	EG/SiO ₂	Temperature (°C)	Time (h)	Products ^a
1	0.01	1.5	200	24	Amor
2	0.04	1.5	200	24	SOD + Amor
3	0.06	1.5	200	24	SOD
4	0.11	1.5	200	24	SOD + Amor
5	0.06	0	200	24	Q + Amor
6	0.06	1.0	200	24	SOD + Amor
7	0.06	1.5	160	24	Amor
8	0.06	1.5	230	12	SOD
9 ^b	0.06	1.5	200	3	SOD

^a The phase appearing first is dominant (Amor: Amorphous; Q: Quartz). ^b The addition of SOD seed in the synthesis system.

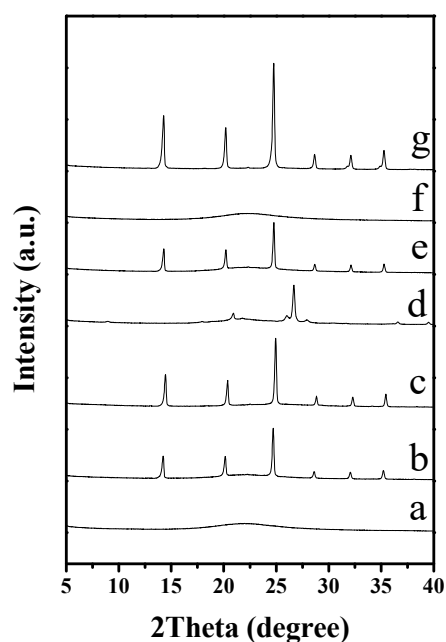


Figure 5. XRD patterns of solid samples synthesized from the starting mixtures with a molar ratio of 1.0 SiO₂/0.01–0.11 Na₂O/0–1.5 ethylene glycol (EG) at 160–230 °C. Na₂O/SiO₂ ratios of (a) 0.01, (b) 0.04, and (c) 0.11; EG/SiO₂ ratios of (d) 0, and (e) 1.0; (f) 160 °C for 24 h; (g) 230 °C for 12 h.

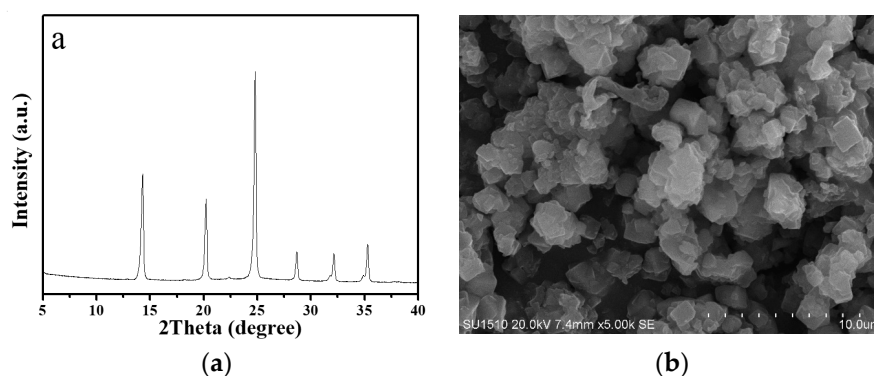


Figure 6. (a) XRD pattern and (b) SEM image of the as-made S–Si–SOD zeolite synthesized at 200 °C.

Based on the aforementioned experimental results, it could be concluded that the synthesis of S-Si-SOD zeolite was greatly influenced by many factors and S-Si-SOD zeolite with high crystallinity could only be obtained in a narrow range of proportions of Na_2O -EG- SiO_2 at an appropriate temperature.

3.3. Crystallization Process of S-Si-SOD Zeolite

In order to understand the synthesis, the crystallization process at 200 °C was characterized by XRD, SEM, UV-Raman, and MAS NMR techniques in detail (Figures 7–10). The photographs of the products before and after crystallization are shown in Figure 11, revealing that the product was always in a solid phase, indicating solvent-free synthesis rather than solvothermal synthesis. The XRD patterns showed that the weak peaks associated with the SOD zeolite structure appeared after crystallization for 12 h (Figure 7c). At the same time, some crystals could be observed via the SEM image (Figure 8b). Increasing the time from 14 to 20 h, the intensity of the peaks gradually increased (Figure 7d–f) and more crystal could be produced (Figure 8c,d). With further increasing the crystallization time to 24 h (Figure 7g), the intensity of the XRD peaks was similar to that of the product crystallized at 20 h, which means that the crystallization was completely finished at 20 h.

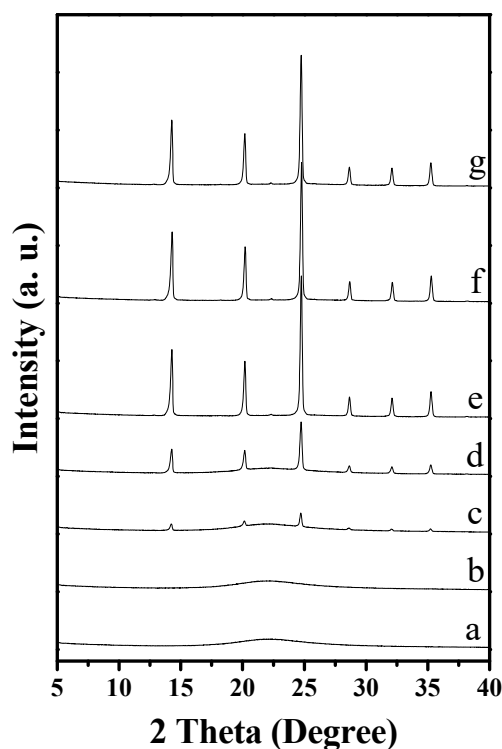


Figure 7. XRD patterns of S-Si-SOD zeolites crystallized at 200 °C for (a) 0, (b) 8, (c) 12, (d) 14, (e) 16, (f) 20, and (g) 24 h, respectively.

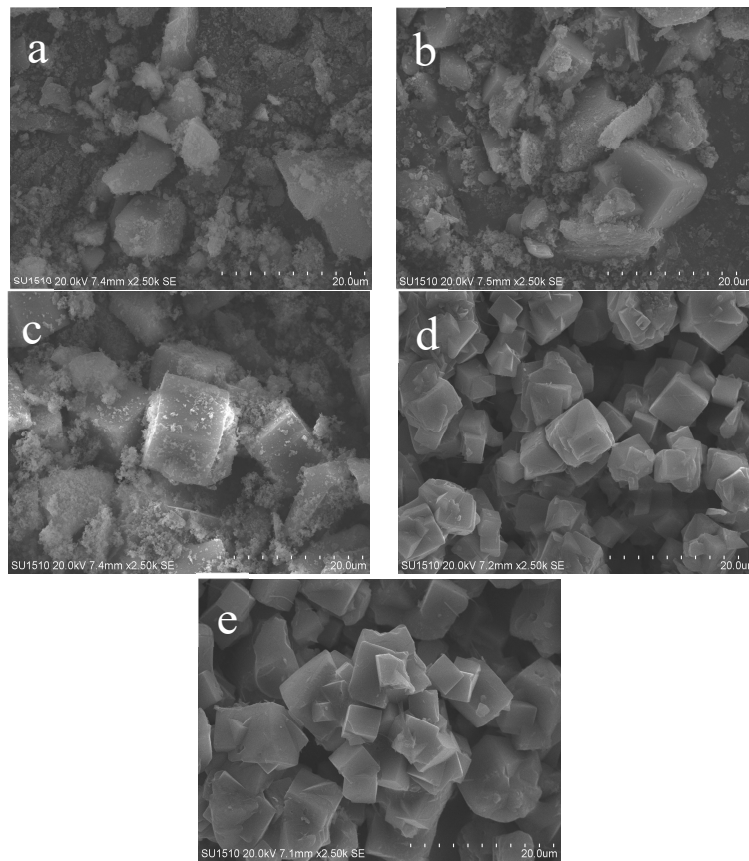


Figure 8. SEM images of S-Si-SOD zeolites crystallized at 200 °C for (a) 0, (b) 12, (c) 14, (d) 16, and (e) 24 h, respectively.

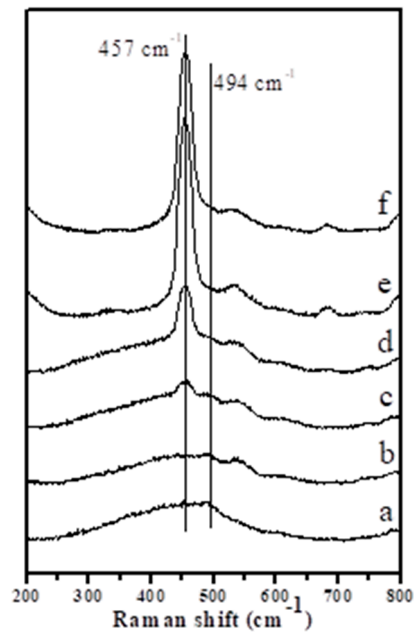


Figure 9. UV-Raman spectra of S-Si-SOD zeolites crystallized at 200 °C for (a) 0, (b) 8, (c) 12, (d) 14, (e) 16, and (f) 24, respectively.

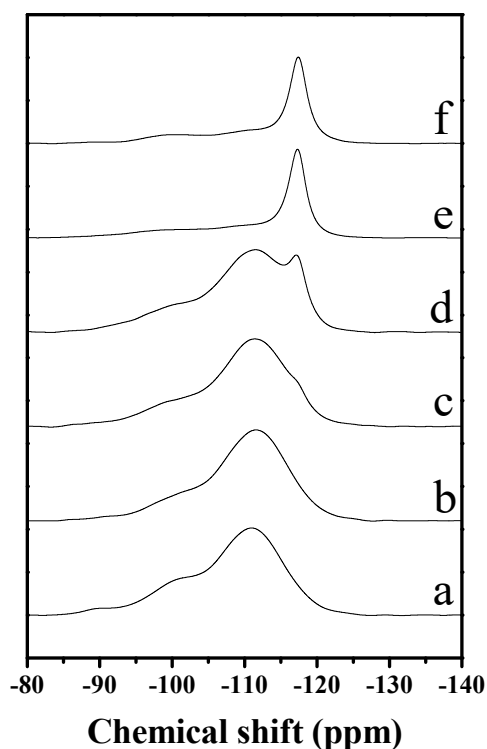


Figure 10. ^{29}Si MAS NMR spectra of S-Si-SOD zeolites crystallized at 200 °C for (a) 0, (b) 8, (c) 12, (d) 14, (e) 16, and (f) 24, respectively.

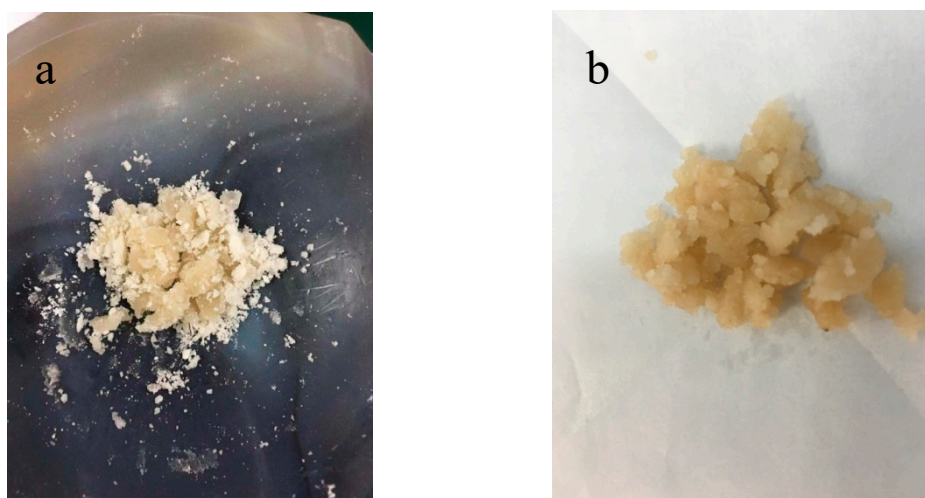


Figure 11. Photographs of the samples (a) before and (b) after crystallization at 200 °C.

Figure 9 showed the UV-Raman spectra of the as-made S-Si-SOD zeolite at various time. Before crystallization, the starting solid mixture exhibited a major broad band at about 494 cm^{-1} , which is assigned to the four-membered rings (4MRs) in the amorphous phase (Figure 9a). After crystallization for 12 h, the product showed the band at about 457 cm^{-1} , which can be reasonably assigned to the 4MRs associated with the SOD zeolite structure (Figure 9c). The intensity of this band increased with the crystallization time, which was in accordance with the SOD zeolite crystallinity (Figure 9d–f). The above result shows that the transformation was from the 4MRs in the amorphous phase to 4MRs in the SOD zeolite structure, suggesting that the 4MRs in the amorphous phase act as be the active building units for the crystallization of S-Si-SOD zeolite.

Figure 10 shows the ^{29}Si MAS NMR spectra of the as-made S–Si–SOD zeolite at various times. Before crystallization, the ^{29}Si MAS NMR spectrum exhibited the main peaks with chemical shifts at about -111.0 and -101.3 ppm, assigned to the Q^4 and Q^3 silica species in the solid silica gel (Figure 10a). As the crystallization time increased, the intensity of the signal peak with the chemical shift at around -117.2 ppm, associated with the Q^4 silica species in the SOD zeolite product, was observed to gradually increase (Figure 10b–f). This indicates the formation of more SOD zeolite crystals, which is in good agreement with the results of the XRD patterns and SEM images. The above results reveal that the condensation of solid silica assisted with EG might be an indication of the formation of the SOD zeolite structure.

4. Conclusions

In summary, we developed a sustainable route to successfully synthesize all-silica S–Si–SOD zeolite under solvent-free conditions. For the first time, S–Si–SOD zeolite was successfully synthesized using this sustainable route. Compared with traditional solvothermal synthesis, the novel route in this work has obvious advantages from the sustainability point of view with respect to high product yield, environment-friendly production, and simple procedures. The above features should open an alternative platform for the efficient synthesis of all-silica SOD zeolite.

Author Contributions: H.Z. and C.B. conceived and designed the experiments; Y.Y. and L.G. performed the experiments; X.W., Q.Y. and J.Z. analyzed the data; L.Z. and X.C. wrote the paper.

Funding: This research was funded by the National Nature Science Foundation of China (21802053 and 21773094) and the University Student Research Innovation Team of Zhejiang Province (2019R417036).

Conflicts of Interest: The authors declare no conflict of interest.

References

1. Wu, Q.M.; Meng, X.J.; Gao, X.H.; Xiao, F.-S. Solvent-free synthesis of zeolites: Mechanism and utility. *Acc. Chem. Res.* **2018**, *51*, 1396–1403. [[CrossRef](#)] [[PubMed](#)]
2. Li, S.Y.; Li, J.F.; Dong, M.; Fan, W.B.; Zhao, T.S.; Wang, J.G.; Fan, W.B. Strategies to control zeolite particle morphology. *Chem. Soc. Rev.* **2019**, *48*, 885–907. [[CrossRef](#)] [[PubMed](#)]
3. Davis, M.E.; Lobo, R.F. Zeolite and molecular sieve synthesis. *Chem. Mater.* **1992**, *4*, 756–768. [[CrossRef](#)]
4. Corma, A. Inorganic solid acids and their use in acid-catalyzed hydrocarbon reactions. *Chem. Rev.* **1995**, *95*, 559–614. [[CrossRef](#)]
5. Wang, Y.; Ren, F.F.; Pan, D.H.; Ma, J.H. A hierarchically micro-meso-macroporous zeolite CaA for methanol conversion to dimethyl ether. *Crystals* **2016**, *6*, 155. [[CrossRef](#)]
6. Cui, Y.C.; Yan, Z.; Li, M.L.; Zhu, J.; Zhu, L.F.; Yao, H.; Cao, X.B. Solvent-free synthesis of all-silica Beta zeolite in the presence of tetraethylammonium bromide. *Crystals* **2018**, *8*, 73.
7. Wu, Q.M.; Hong, X.; Zhu, L.F.; Meng, X.J.; Han, S.H.; Zhang, J.; Liu, X.L.; Jin, C.H.; Xiao, F.S. Generalized ionothermal synthesis of silica-based zeolites. *Microporous Mesoporous Mater.* **2019**, *286*, 163–168. [[CrossRef](#)]
8. Vattipalli, V.; Paracha, A.M.; Hu, W.G.; Chen, H.Y.; Fan, W. Broadening the scope for fluoride-free synthesis of siliceous zeolites. *Angew. Chem. Int. Ed.* **2018**, *57*, 3607–3611. [[CrossRef](#)] [[PubMed](#)]
9. Liu, X.L.; Luo, Q. Solid state NMR spectroscopy studies of the nature of structure direction of OSDAs in pure-silica zeolites ZSM-5 and Beta. *J. Phy. Chem. C* **2017**, *121*, 13211–13217. [[CrossRef](#)]
10. Zhu, Z.G.; Xu, H.; Jiang, J.G.; Wu, H.H.; Wu, P. Hydrophobic nanosized all-silica Beta zeolite: Efficient synthesis and adsorption application. *ACS Appl. Mater. Interfaces* **2017**, *9*, 27273–27283. [[CrossRef](#)] [[PubMed](#)]
11. Zhang, L.; Jiang, Y.W.; Chen, B.B.; Shi, C.; Li, Y.B.; Wang, C.Y.; Han, S.C.; Pan, S.X.; Wang, L.; Meng, X.J.; et al. Exceptional activity for formaldehyde combustion using siliceous Beta zeolite as a catalyst support. *Catal. Today* **2019**. [[CrossRef](#)]
12. Liu, Y.T.; Tian, T. Fabrication of diatomite/silicalite-1 composites and their property for VOCs adsorption. *Materials* **2019**, *12*, 551. [[CrossRef](#)] [[PubMed](#)]

13. Lew, C.M.; Li, Z.J.; Li, S.; Hwang, S.J.; Liu, Y.; Medina, D.I.; Sun, M.W.; Wang, J.L.; Davis, M.E.; Yan, Y.S. Pure-silica-zeolite MFI and MEL low-dielectric-constant films with fluoro-organic-functionalization. *Adv. Funct. Mater.* **2008**, *18*, 3454–3460. [[CrossRef](#)]
14. Bibby, D.M.; Dale, M.P. Synthesis of silica-sodalite from non-aqueous systems. *Nature* **1985**, *317*, 157–158. [[CrossRef](#)]
15. Yang, X.B.; Albrecht, D.; Caro, J. Solvothermal synthesis and silica-sodalite: Effects of water, germanium and fluoride. *Microporous Mesoporous Mater.* **2007**, *100*, 95–102. [[CrossRef](#)]
16. Zhang, S.Q.; Cui, M.; Zhang, Y.F.; Zheng, J.Q.; Lv, T.M.; Gao, W.Y.; Liu, X.Y.; Meng, C.G. Study on the synthesis of FER and SOD in the presence of ethylene glycol and the oxidation transformation of ethylene glycol in a confined region of zeolites. *J. Alloys Compd.* **2017**, *244*, 158–163. [[CrossRef](#)]
17. Werthmann, U.; Marler, B.; Gies, H. Pyrrolidine silica sodalite and ethylamine sodalite-two new silica sodalite materials synthesized from different solid silica sources. *Microporous Mesoporous Mater.* **2000**, *39*, 549–562. [[CrossRef](#)]
18. Morris, R.E.; James, S.L. Solventless synthesis of zeolites. *Angew. Chem. Int. Ed.* **2013**, *52*, 2163–2165. [[CrossRef](#)] [[PubMed](#)]
19. Wu, Q.M.; Wang, X.; Qi, G.D.; Guo, Q.; Pan, S.X.; Meng, X.J.; Xu, J.; Deng, F.; Fan, F.T.; Feng, Z.C.; et al. Sustainable synthesis of zeolites without addition of both organotemplates and solvents. *J. Am. Chem. Soc.* **2014**, *136*, 4019–4025. [[CrossRef](#)] [[PubMed](#)]
20. Zhu, L.F.; Zhang, J.; Wang, L.; Wu, Q.M.; Bian, C.Q.; Pan, S.X.; Meng, X.J.; Xiao, F.S. Solvent-free synthesis of titanosilicate zeolites. *J. Mater. Chem. A* **2015**, *3*, 14093–14095. [[CrossRef](#)]
21. Yu, X.; Zhou, C.H.; Chen, X.Q.; Gao, P.; Qiu, M.H.; Xue, W.J.; Yang, C.G.; Zhao, H.Q.; Liu, H.J.; Liu, Z.Y.; et al. Facile solvent-free synthesis of hollow fiber catalyst assembled by c-axis oriented ZSM-5 crystals. *ChemCatChem* **2018**, *10*, 5619–5626. [[CrossRef](#)]
22. Gao, W.Z.; Amoo, C.C.; Zhang, G.H.; Javed, M.; Mazonde, B.; Lu, C.X.; Yang, R.Q.; Xing, C.; Tsubaki, N. Insight into solvent-free synthesis of MOR zeolite and its laboratory scale production. *Microporous Mesoporous Mater.* **2019**, *280*, 187–194. [[CrossRef](#)]



© 2019 by the authors. Licensee MDPI, Basel, Switzerland. This article is an open access article distributed under the terms and conditions of the Creative Commons Attribution (CC BY) license (<http://creativecommons.org/licenses/by/4.0/>).